HPV in situ hybridization: impact of different protocols on the detection of integrated HPV.

Int. J. Cancer: **115,** 419–428 (2005)

HPV *in situ* hybridization: impact of different protocols on the detection of integrated HPV

Anton H.N. Hopman [1]*, Miriam A. Kamps[1], Frank Smedts[2], Ernst-Jan M. Speel[1], C. Simon Herrington[3] and Frans C.S. Ramaekers[1]

[1]*Department of Molecular Cell Biology, Research Institute Growth and Development (GROW), University of Maastricht, The Netherlands*
[2]*Department of Pathology, Foundation of Collaborating Hospitals of Eastern Groningen (SSZOG), Winschoten, The Netherlands*
[3]*Bute Medical School, University of St. Andrews, St. Andrews, United Kingdom*

Although there is consensus that HPV integration is common in invasive cervical carcinomas and uncommon or absent in low-grade uterine cervical intraepithelial neoplasia (CIN I), estimates for HPV integration in CIN II/III range from 5 to 100% using different PCR-based and *in situ* hybridization (ISH) approaches. It has been suggested that HPV integration can be identified using ISH by scoring of punctate signals. The increased sensitivity of fluorescence ISH (FISH) methods, allowing the detection of single copies of HPV, complicates the distinction between integrated and episomal HPV. Recently it has been suggested that, in such assays, the signals originating from integrated virus can be hidden in a background of episomal HPV. We therefore compared 2 different FISH protocols for the detection of integrated HPV in a series of CIN II/III lesions: 1) a mild protocol in which episomal HPV and RNA is retained and 2) a harsh protocol that extensively extracts proteins and RNA, and which promotes the partial loss of episomal HPV but not integrated HPV. A series of 28 HPV 16/18 positive CIN II/III lesions (17 solitary lesions and 11 lesions adjacent to microinvasive carcinoma) were studied. A punctate signal pattern was identified in 7 of these lesions with both protocols. Punctate signal was also present in control samples from lesions that are known to be associated with HPV integration (invasive squamous cell carcinoma ($n = 3$), adenocarcinoma in situ ($n = 3$), and invasive adenocarcinoma ($n = 1$). HPV RNA contributed significantly to the intensity of punctate FISH signal, especially when applying the mild protocol, as shown by omitting DNA denaturation, including RNase pretreatment steps and measuring the fluorescence signal intensity. Also, HPV RNA was frequently detected in addition to episomal/integrated HPV DNA in the majority of the other 21 CIN II/III lesions; this resulted in intense granular/diffuse FISH signals throughout the epithelium. However, in 7 of these lesions, the harsh protocol gave a more consistent punctate pattern in cells throughout the full thickness of the epithelium. This supports the hypothesis that the harsh protocol unmasks integrated HPV more efficiently by extracting RNA and episomal HPV. Overall, with this harsh protocol, a clonally expanded population of cells containing punctate HPV signals was found in 5 of 17 (29%) solitary CIN II/III lesions and in 9 of 11 (88%) CIN II/III lesions associated with microinvasive carcinoma. Combining these data with the results from our previous study, with the harsh protocol in 7 of 40 (18%) solitary CIN II/III lesions and 19/21 (90%) CIN II/III lesions associated with microinvasive carcinoma ($p < 0.001$), this pattern was found. This indicates that, when robustly defined, a punctate HPV pattern in CIN II/III lesions is associated with the presence of an invasive carcinoma.

Key words: uterine cervix; dysplasia; SIL; CIN; HPV 16/18; HPV integration; chromosomal aberrations

Several premalignant stages can be distinguished in the development of carcinoma of the uterine cervix. These include cervical intraepithelial neoplasia grades I, II and III (CIN I–III), also designated low-grade squamous intraepithelial lesions (LSIL, comprising CIN I) and high grade SIL (HSIL, comprising CIN II-III).[1–4] Nearly all invasive cervical carcinomas (ICCs) and CIN grade II/III lesions contain human papillomavirus (HPV) DNA. Epidemiological studies indicate that HPV is without doubt the most important factor in the carcinogenic process of the uterine cervix. It has been estimated that 80% of women acquire an HPV infection at some point during their lifetime, but that the majority of these infections are transient, with only a minority ever resulting in recognizable CIN III. The vast majority of CIN I lesions regress spontaneously, and only very few lesions persist or progress to CIN II–III. One factor considered to be of key importance for the progression of intraepithelial lesions to invasive disease is integration of HPV into the host cell genome.[2,7–9] The majority of CIN II/III lesions and all ICCs are infected with high risk (oncogenic) HPV types, particularly HPV 16 and 18. The *E2* region of the HPV genome, which is involved in the regulation of the oncogenic HPV E6 and E7 proteins, is frequently disrupted when the virus is integrated.[2,4,10,11] In the majority of cases this results in constant suppression of key cell-cycle control proteins p53 and pRB by the HPV *E6* and *E7* gene products, respectively. There is a consensus that integration is common in ICC and most studies indicate that integration is uncommon or absent in CIN I.

In reviewing the literature, Evans and Cooper[12] commented on the wide range of estimates for integration in CINII/III, *i.e.*, 5 to 100% as determined by means of Southern blot assays, different types of PCR analyses, as well as chromogenic and fluorescence in situ hybridization methods (FISH).[13–18] They concluded that, although questions remain regarding the prevalence of integration in preinvasive lesions, ISH approaches may be a viable alternative to PCR in determining both infection with high risk HPV as well as its physical status.

The first assays to detect integrated HPV were based on restriction digestion/Southern blot hybridization.[19] Comparison of ISH signal patterns with these assays demonstrated that a punctate pattern, consisting of 1 or a few discrete signal(s) in the nucleus, indicates HPV integration into the cellular genome. A diffuse nuclear pattern on the other hand represents multiple copies of episomal HPV and correlates with viral replication.[19] These early ISH methods were based on moderately sensitive approaches but, in the last decade, numerous more sensitive (F)ISH assays have been developed that allow the detection of a single-copy of HPV.[17,20–24] Applying these sensitive methods to CIN II/III lesions results, however, in an increase in the number of FISH signals within individual nuclei. The inherent problem of this approach is that signals originating from integrated HPV can be hidden in a background of episomal copies. Furthermore, HPV can also be present as concatamers, which makes the recognition of integrated HPV even more difficult.[12] Moreover, HPV RNA can contribute to the signals observed in these (F)ISH protocols.[25,26]

In our study, we determined the impact of different protocols for the identification of HPV by FISH with respect to signal distribution throughout the epithelium, signal pattern (diffuse/punctate/

***Correspondence to:** Department of Molecular Cell Biology (Box 17), University of Maastricht, PO Box 616, 6200 MD Maastricht, The Netherlands. Fax: +31-43-3884151.
E-mail: Hopman@molcelb.unimaas.nl
Received 24 August 2004; Accepted after revision 28 October 2004
DOI 10.1002/ijc.20862
Published online 1 February 2005 in Wiley InterScience (www.interscience.wiley.com).

granular) and contribution of HPV RNA to the final hybridization signal. For this purpose we compared a frequently used HPV detection method that employs a mild pretreatment protocol to a protocol that we developed for the visualization of chromosomal targets.[27,28] These chromosomal targets need harsh pretreatment steps to open chromosomal sites for efficient hybridization and immunocytochemical detection. The latter protocol has been shown to remove most of the cytoplasmic as well as nuclear proteins and has been hypothesized to extract episomal HPV copies.[12] Here we report that application of this protocol results in the partial extraction of episomal HPV as well as HPV RNA, resulting in better recognition of a punctate pattern indicative of integrated HPV.

Materials and methods

Tissue material

Formalin-fixed and paraffin wax-embedded endo/ectocervical biopsies, diathermy loop excisions and cold knife cervical conization samples were selected from the files of the Department of Pathology, Foundation of Collaborating Hospitals of Eastern Groningen, Winschoten, The Netherlands. The cervical biopsies were classified independently according to WHO criteria by 2 pathologists (FS and CSH), after which all cases were reviewed together and cases with discrepancy discussed until consensus was reached. Invasion was classified according to FIGO staging criteria. Thirty-two CIN II/III lesions were selected; 19 lesions showed no evidence of an invasive carcinoma (consecutive cases of CIN II/III), while 13 CIN III lesions were associated with a microinvasive carcinoma (consecutive cases of CIN II/III&mCA). The lesions were processed in such a way that they were gathered on 3 slides. This small tissue micro array allowed a comparison of hybridisation results (quantified by measuring the fluorescence intensity) because all lesions were simultaneously processed including the enzymatic (peroxidase) signal amplification reaction. A small series of controls was selected that were predicted to contain integrated HPV; these included 3 squamous carcinomas, 1 adenocarcinoma and 3 adenocarcinomas *in situ* (ACIS). All ACIS were HPV 18 positive: HPV DNA (notably HPV 18) is usually present in the integrated form in endocervical neoplasia.[29]

Ki-67 and p16^{ink4a} *immunohistochemistry*

Four micrometer thick tissue sections were dewaxed and immuno stained as described previously. Briefly, after deparaffinization sections were pretreated with 0.3% H_2O_2 in methanol to quench endogenous peroxidase activity, followed by antigen retrieval using microwave heating at 100°C in 0.01 M citrate buffer (pH 6.0) for 30 min (interval micro waving). The Ki-67 (Immunotech, Marseille, France) and p16^{ink4a} (E6H4, DAKO A/S, Denmark) were detected by incubating the slides subsequently with the monoclonal antibodies (according to the instructions of the supplier), biotinylated rabbit anti-mouse IgG (1:200, Vector Laboratories, Burlingame, CA) and an avidin-biotinylated peroxidase complex (ABC) (Vectastain PK4000, Vector Laboratories, Burlingame, CA). Peroxidase activity was visualized using diaminobenzidine (DAB)/H_2O_2 and sections were counterstained with haematoxylin and mounted in Entellan (Merck, Darmstadt, Germany).

Fluorescence in situ *hybridization*

Probe selection and labeling procedures. Digoxigenin-labeled HPV 16 and HPV 18 probes were purchased from PanPath, Amsterdam, The Netherlands and used as a mixture (HPV 16/18) for primary screening. Probes for chromosomes 1 (1q12),[30] and 17 (17 alphoid centromere sequence)[31] were selected to determine hybridisation efficiency and reproducibility on chromosomal targets, and used to determine chromosomal aneusomy. The probes were labeled by standard nick translation with biotin (Bio)- or digoxigenin (Dig)-dUTPs. For multiple target analyses the following probe combination was used: chrom 1-Bio and chrom 17-Dig.

Pretreatment protocols. Two different pretreatment protocols were used. The mild procedure includes a simple pepsin incubation step in 0.2 N HCl combined with high temperature denaturation.[13] The harsh procedure includes 2 chemical (acid and protein denaturation) soaking steps and a pepsin incubation step in 0.02 N HCl.[28,32] The sensitivity and reliability of the harsh protocol for HPV was described previously by testing HPV positive cell lines (SiHa, Hela and Caski) and screening of routine fixed head and neck lesions and cervical preneoplasia.[17,21]

Mild pretreatment. Four micrometer thick paraffin wax tissue sections were dewaxed and digested with 8 mg/ml pepsin (800–1,200 U/mg protein porcine stomach mucosa; Sigma Chemical Co., St. Louis, MO) in 0.2 M HCl for 10 min at 37°C. The slides were rinsed 3 times in H_2O and dehydrated in an ascending ethanol series. After air drying the HPV probe set was applied under a coverslip (see below). Probe and target DNA were denatured simultaneously for 6 min at 90°C prior to hybridisation. When target denaturation was omitted, the probe was denatured separately in an eppendorf tube for 10 min at 80°C and chilled on ice prior to application to the tissue section under a coverslip. For RNase treatment, the slides were dewaxed and incubated for 10 min at 80°C in 2 × SSC, rinsed in H_2O at room temperature and dehydrated in an ascending ethanol series. They were then incubated in 4 mg/ml DNase free RNase (Roche, Mannheim, Germany) in 10 mM TrisHCl, 1 mM EDTA pH 7.5 for 60 min at 37°C.

Harsh pretreatment. Four micrometer thick paraffin wax tissue sections were dewaxed, pre-treated with 85% formic acid/0.3% H_2O_2 for 20 min at room temperature, and subsequently dehydrated with 70% ethanol containing 0.01 M HCl (acid dehydration), 90% ethanol and 100% ethanol for 3 min each prior to air drying. The slides were incubated in 1 M NaSCN for 10 min at 80°C, followed by acid dehydration and digestion with 4 mg/ml pepsin (800–1,200 U/mg protein porcine stomach mucosa: from Sigma Chemical Co., St. Louis, MO) in 0.02 M HCl for 15 min at 37°C. The slides were rinsed 3 times in 0.01 M HCl and acid dehydrated. After air drying sections were post-fixed in 1% formaldehyde in PBS for 15 min at room temperature, rinsed 3 times in PBS and dehydrated in an ascending ethanol series.

The chemical pretreatment steps (formic acid/hydrogen peroxide, and thiocyanate at 80°C) in combination with pepsin treatments remove nearly all nuclear and cytoplasmic proteins. This procedure strongly improves the hybridisation efficiency, maintains nuclear morphology during the FISH procedure and reduces the need for optimization of the digestion time for each sample.[32] The chemical pretreatment steps in the harsh protocol lead to partial denaturation of DNA (thiocyanate is a DNA denaturing agent); application of this pretreatment step therefore does not enable a valid evaluation of the contribution of RNA hybridization when applying this pretreatment step.

The low level of autofluorescence of cytoplasmic and nuclear protein remnants after application of the harsh protocol indicates that these proteins have been efficiently removed. In the mild protocol, nuclear and cytoplasmic autofluorescence is frequently greater, indicating that these proteins are at least partially retained. In particular, the latter will have impact on the retention of RNA in both cytoplasm and nucleus.

The probe sets were applied under a coverslip at a concentration of 1 ng/μl in 60% formamide, 2 × SSC, 10% dextran sulfate and 50 × excess of carrier DNA (salmon sperm DNA). Probe and target DNA were denatured simultaneously for 5 min at 80°C prior to hybridization overnight at 37°C. After hybridization the preparations were washed stringently in 50% formamide, 2 × SSC at 42°C (2 times 5 min) or 0.1 × SSC at 61°C (2 times 5 min).

Probe detection and microscopic imaging. The digoxigenin (Dig)-labeled HPV probes were detected using the tyramide signal amplification (TSA) procedure as previously described for single target hybridisation using rhodamine-labeled tyramide.[33] In short, the Dig-labeled probe was detected by peroxidase-conjugated sheep anti-digoxigenin Fab fragments (SHaDIG-PO, 1:100; Roche

TABLE I – SUMMARY OF SEMI-QUANTITIVE EVALUATION OF IN SITU HPV SIGNALS USING A X40 DRY OBJECTIVE[1]

Group	Case	Age	CIN lesion	HPV tested	Staining patterns					
					mild protocol			harsh protocol		
					Diffuse	Granular	Punctate	Diffuse	Granular	Punctate
A	1	38	III	16/18	■			◩		
	2	32	III&mCA	16/18	■			□		
	3	36	III	16/18	■	■		□		
	4	24	III	16/18	■	■		◩		
	5	29	III	16/18	■	■		□		
	6	28	III	16/18	■	■		◩	◩	
	7	35	III	16/18	■	■		■		
	8	41	III	16/18	■	■		◩		
	9	37	III	16/18	■	■		■	◩	
	10	31	II	16/18		■		◩		
	11	22	III	16/18		■		□	□	
	12	34	II/III	16/18		■		■		
	13	31	III	16/18		■		□	◩	
	14	36	II&mCA	16/18		■		□		
B	15	38	III&mCA	16/18		■		□	□	□
	16	34	III&mCA	16/18		■				◩
	17	41	III&mCA	16/18	■	■				◩
	18	n.a	III	16/18	■	■		■		■
	19	40	III&mCA	16/18	◩	■			□	◩
	20	39	III	16/18		■				◩
	21	47	III&mCA	16/18		■				◩
C	22	30	III	16/18	■	■	◩	■		◩
	23	38	III&mCA	16/18		■	◩			◩
	24	43	III&mCA	16/18			◩			■
	25	37	III	16/18			■			◩
	26	30	III	16/18			■			◩
	27	48	III&mCA	16/18			■			■
	28	30	III&mCA	16/18			■			■
	29	35	squam. CARC	16/18			■			■
	30	n.a	squam. CARC	16/18		n.d.				■
	31	n.a	squam. CARC	16/18		n.d.				■
	32	35	ACIS	18			■			◩
	33	n.a	ACIS	18		n.d.				■
	34	32	ACIS	18		n.d.				■
	35	40	adeno CARC	18			■			◩

[1]Highest intensity indicated by ■, intermediate intensity by ◩, and lowest intensity by □. The criteria for assessment of signal type are given in Material and methods. n.a: not available, n.d: not done.

Molecular Chemicals, Basel, Switzerland) or first mouse anti-digoxigenin (MaDig, 1:2,000 Sigma Chemical Co.), then a peroxidase-conjugated rabbit anti-mouse (RaM-PO, 1:100 DAKO A/S Glostrup, Denmark) and finally a peroxidase-conjugated swine anti-rabbit (SwaR-PO, 1:100 DAKO) all for 30 min incubatoons at 37°C, and washed in PBS/0.05% Tween-20. Thereafter, the TSA amplification reaction was carried out under a coverslip by applying 50 ml (1:500 diluted from a 1 mg/ml stock solution in ethanol) rhodamine-labeled tyramide in PBS containing 0.1 M imidazole, pH 7.6, and 0.001% H_2O_2 for 10 min at 37°C. The slides were washed in PBS containing 0.05% Tween-20 (Janssen Chimica, Beerse, Belgium), dehydrated in an ascending ethanol series and mounted in Vectashield (Vector Laboratories) containing 4′,6-diamidino-2-phenylindole (DAPI; Sigma Chemical Co.: 0.5 ng/μl).

Comparison of conventional cytochemical detection systems and TSA systems have shown that, especially with the latter system, both specific and nonspecific (background) ISH signals may be greatly amplified. It is essential to keep nonspecific probe binding and detection at a minimum for routine application of the method. Many parameters have been shown to have impact on the signal-to-noise (S/N) ratio when applying the TSA method including, *e.g.*, probe and detection conjugate concentration, type of tyramide, amplification buffer, reaction time and reaction temperature.[34]

The biotin (Bio) labeled centromeric probe was detected with sequential incubations with fluorescein isothiocyanate (FITC) conjugated avidin (AvFITC, 1:100; Vector, Brunswig Chemie, Amsterdam, The Netherlands), biotin conjugated goat anti-avidin (BioGaA, 1:100 Vector Laboratories) and FITC-conjugated avidin 1:100, all for 20 min at 37°C , diluted and washed in 4 × SSC/0.05% Tween-20 (Janssen Chimica, Beerse, Belgium). The following series of incubations were used to detect the Dig-labeled centromeric probe: first mouse anti-digoxigenin (MaDig, 1:2,000; Sigma Chemical Co.), then rhodamine (TRITC) conjugated rabbit anti-mouse (RaMTRITC, 1:1,000 Sigma Chemical Co.) and finally TRITC-conjugated swine anti-rabbit (SwaRTRITC, 1:100 DAKO A/S Glostrup, Denmark), all for 30 min at 37°C, diluted and washed in PBS/0.05% Tween-20. After detection, the slides were dehydrated in an ascending ethanol series and mounted in Vectashield (Vector Laboratories) containing 4′,6-diamidino-2-phenylindole (DAPI; Sigma Chemical Co.: 0.5 ng/μl).

Imaging. Images were recorded with the Metasystems Image Pro System (black and white CCD camera; Sandhausen, Germany) mounted on a Leica DM-RE fluorescence microscope equipped with FITC, TRITC, DAPI and SpectrumGold single bandpass filters for single color analysis and a triple bandpass filter set (FITC, TRITC and DAPI) for simultaneous dual- and triple-color analysis. Images were recorded using an automatic integration time allowing quantitative measurements (using the full dynamic range of the camera without signal intensity saturation; TIF 8 bits image). Furthermore, fixed integration times were used to compare fluorescence intensity between different preparations.[35] FISH fluorescence was measured per area or per individual nucleus using Image/J (http://www.nih.gov, public domain), after color separation (RGB split), thresholding and selection of regions of interest.

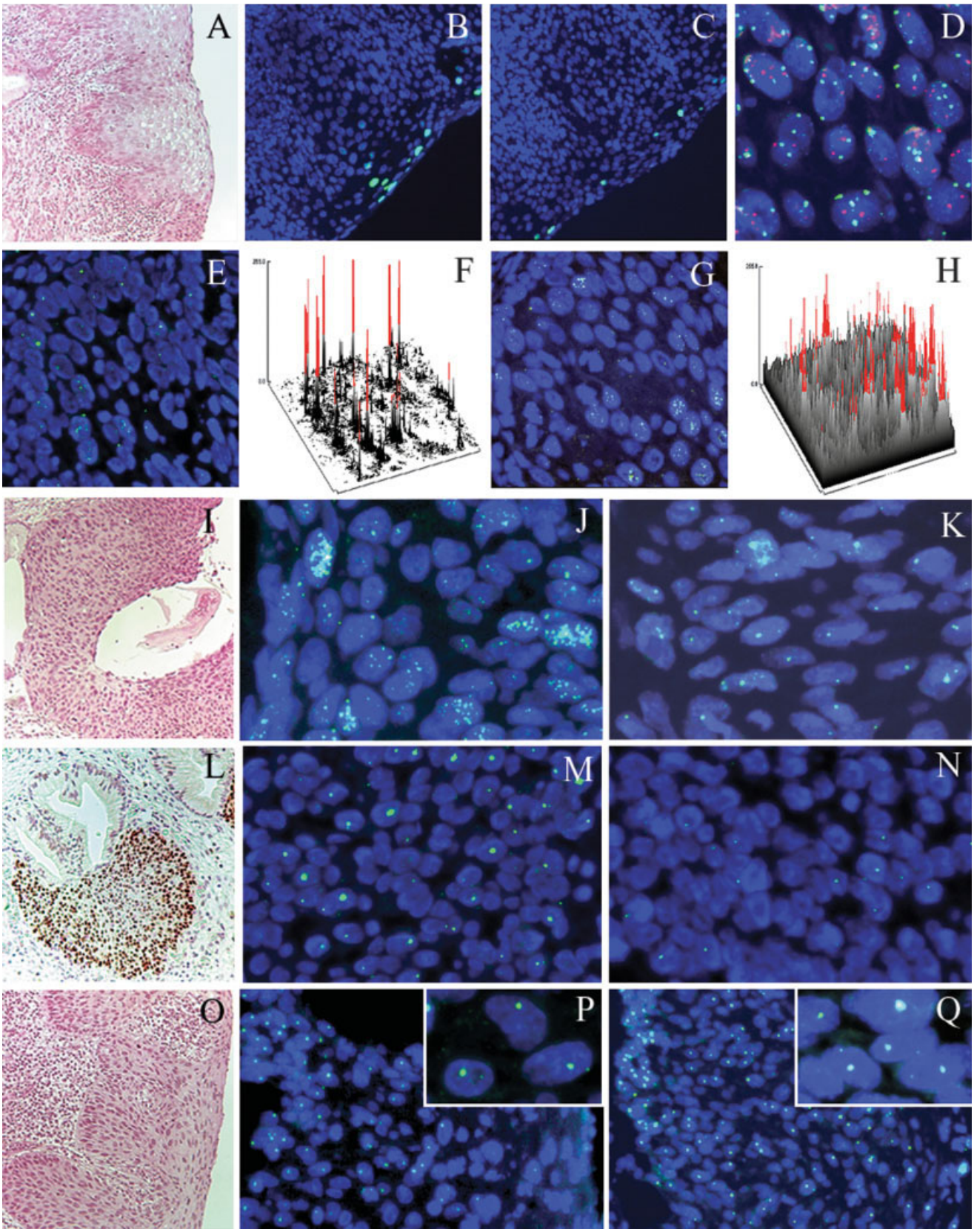

FIGURE 1.

Signal intensity (spot or nucleus) was calculated as mean signal intensity (per pixel) times area.

To compare the impact of the different protocols and/or pretreatment steps on FISH signal distribution throughout the epithelium, only samples that were processed simultaneously were compared. Furthermore lesions were collected on small tissue arrays that enabled identical processing of different lesions.

Controls and evaluation of FISH results. Controls included HPV-16 and -18 hybridization on tissue sections of formalin fixed and paraffin wax-embedded HPV positive cell lines (SiHa, CaSki and HeLa). Evaluation of nuclear hybridization signals was performed by 3 investigators (A.H., M.K. and C.H). Signal morphology was categorized as follows: 1) When nuclei were completely and homogeneously stained, the signal was classified as diffuse. Often, the other nuclei exhibited multiple fluorescent signals with variation in spot number between individual cells within the lesion; 2) When nuclear signals varied significantly in size and intensity this pattern was termed granular[13] and 3) Discrete nuclear signals (1–3 per nucleus) in a clean background were classified as punctate, in line with the criteria of Cooper *et al.*[19]

The method was tested on 4 μm thick formalin fixed and paraffin wax-embedded CaSki and SiHa cell lines that contain approximately 500 and 2 copies of integrated HPV 16, respectively.[17] The FISH procedure as described above, guarantees an optimal signal-to-noise ratio.[17,33,36] In particular with the fluorescent TSA method, noise is often present as a result of background reactions which could be misclassified as viral particles. Histological HPV negative areas (*e.g.*, lymphocytes) served as internal controls to estimate specific and nonspecific signal.

Results

Ki-67 and p16^{INK4a} *immunohistochemistry*

The Ki-67 index was mainly utilized for verification of the different histological entities and served as a landmark in brightfield microscopy to guide evaluation of the FISH patterns. All cervical lesions positive for p16^{INK4a} exhibited strong nuclear and cytoplasmic immuno staining in the premalignant areas. FISH HPV-positivity correlated strongly with p16^{INK4a} accumulation, but not all p16^{INK4a} positive cells showed a FISH signal for HPV 16/18 DNA.

Distribution of HPV 16/18 FISH signals in (pre)malignant lesions

The results of the HPV FISH reactions for the 2 protocols are summarized in Table I, and typical examples are depicted in Figure 1. In total, 32 high grade CIN II/III lesions were examined for the FISH distribution patterns of HPV after applying the 2 different protocols. HPV 16/18 positivity was detected in 17 CIN II/III lesions and in 11 CIN II/III lesions adjacent to microinvasive carcinomas. Four lesions were HPV 16/18 FISH negative (in both protocols) and most likely contain other HPV types (not determined). In the control group, cases were compared after applying the 2 different protocols.

The results were obtained by visual evaluation of the FISH signal intensity. No imaging by means of the CCD camera was needed for this classification. Intensity differences obtained for both protocols were compared for individual lesions within identical areas on serial sections. The absolute fluorescence intensity of the signals varied within a relatively wide range between individual lesions, which results in a range of capture times (automated integration time, range 0.1–3 sec, average about 0.3 sec) using the CCD camera for imaging. This variation does not influence the classification upon visual inspection.

In general the mild protocol resulted in HPV signals of higher fluorescence intensity than the harsh protocol. The lesions were grouped according to the major types of HPV distribution pattern. In lesions 1–14 (group A), only diffuse and/or granular patterns were recognized when applying both pretreatment protocols. In lesions 15–21 (group B), the patterns obtained with the 2 protocols were clearly discordant. Only punctate patterns were recognized with the harsh protocol, while the mild protocol showed a granular pattern in all cases. In half of these cases, this granular pattern was combined with a diffuse pattern. In cases 22–35 (group C), the majority of the lesions showed the typical punctate pattern with both protocols.

Cases 1–14 (group A). In this group, the nuclei with a diffuse pattern were predominantly found in the superficial layers. A diffuse pattern is illustrated for the mild and harsh protocol in Figure 1*b*,*c* (case 2). In this case, strongly fluorescent signals were present in individual cells of the basal part of the epithelium with the mild protocol (compare Fig. 1*e*,*g*). In Figure 1*b*,*c*, these signals in the lower compartment cannot be seen because of their small size, which is below the resolution of this image. A typical diffuse and granular pattern from this group after application of the mild protocol is depicted in Figure 1*j*.

In this group, a similar pattern was obtained using both methods. Overall the HPV FISH signal intensities for the mild protocol were higher in these lesions than the signals obtained with the harsh protocol in 11 of 14 cases. Quantitative measurements of the fluorescence intensity in nuclei in the superficial layer of case 2 revealed about 30-fold higher signal intensity compared to the basal/parabasal cell nuclei (Fig. 2*a*). This difference is attributed to viral replication in superficial layers and low viral copy number in the basal/parabasal layers. The intensity obtained with the harsh protocol in the superficial layers of this case was 15-fold lower than the intensity measured for the mild protocol.

These differences in signal intensity support the hypothesis that the harsh protocol leads to removal of episomal HPV copies as a result of the more aggressive removal of cytoplasmic and nuclear constituents. Moreover, the contribution of HPV RNA hybridization to the signal might be considerable and this was studied by omission of target DNA denaturation and by application of RNase digestion followed by DNA denaturation. When denaturation of the target DNA was omitted, resulting in the detection of only RNA, strong signals were seen in the lower compartment of the epithelium (Fig. 1*e*). A surface plot of the fluorescence intensity in the lower part of the epithelium (Fig. 1*f*) illustrates the high intensity of these signals in a relatively low background. We conclude that these signals originate from RNA because the signals disappeared when an RNase pretreatment step was included in the protocol (results not shown). However, if a denaturation step was included after RNase pretreatment, these areas exhibited multiple small signals, representing HPV DNA (Fig. 1*g*). The number of HPV DNA spots per nucleus increases towards the more superfi-

FIGURE 1 – Representative examples of tissue sections from patients diagnosed with cervical intraepithelial neoplasia stained with haematoxylin (*a*,*i*,*o*), analyzed by FISH for oncogenic type HPV 16/18 shown in green (*b*,*c*,*e*,*g*,*j*,*k*,*m*,*n*,*p*,*q*), a double target hybridization on chromosomes 1 and 17 (*d*) and immunohistochemical staining for p16^{ink4a} (*i*). (*a-h*) (case 2): HPV analysis of a CIN II/III lesion with the mild protocol (*b*) and the harsh protocol (*c*). (*e*) and (*g*) Results obtained with the mild protocol without DNA denaturation (*e*) or with RNase treatment prior to DNA denaturation (*g*). (*d*) Double target hybridization on chromosomes 1 and 17 developed in green (FITC) and red (TRITC) fluorescence, respectively. Nuclear counterstaining in FISH experiments was with DAPI (blue). (*f*,*h*) Surface fluorescence intensity plots of (*e*) and (*g*), respectively. These plots illustrate the high level of signal to noise ratio and distribution of the spots within the individual nuclei. (*i–k*) (case19): CIN III lesion analyzed with the mild protocol (*j*) and the harsh protocol (*k*). In the mild protocol, there are superimposed signals apparently originating from HPV RNA and/or episomal HPV.(*l–n*) (case 26): CIN III lesion immunohistochemical staining for p16^{ink4a} (*i*) and HPV detection using the mild protocol either by omitting DNA denaturation (*m*) or RNase treatment followed by a target denaturation (*n*). (*o–q*) (case 28): CIN III area (CINIII&mCA) analyzed with the mild protocol (*p*) or the harsh protocol (*q*). Higher magnifications (inserts) show nuclei with 1 strong and 1 weak HPV signal in both protocols.

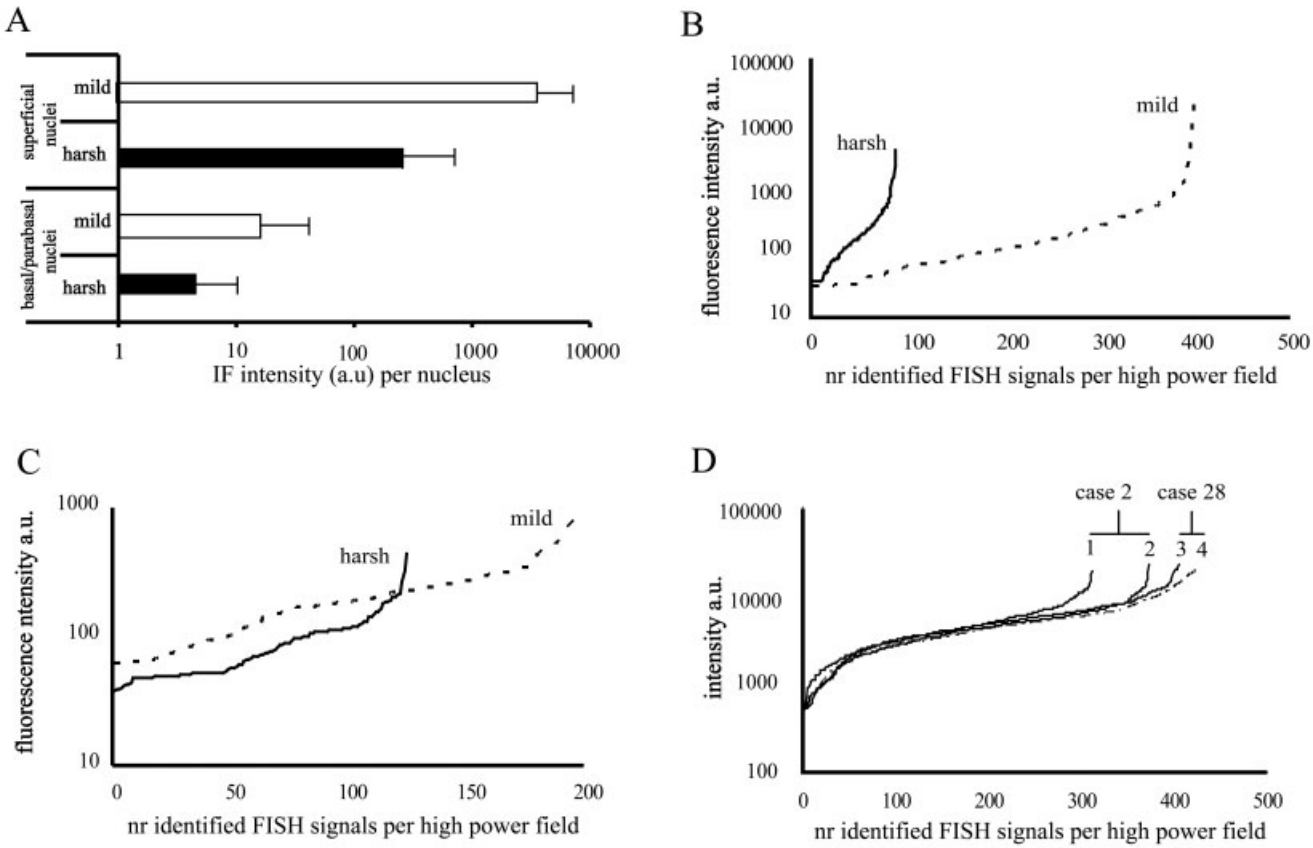

Figure 2 – Quantitative fluorescence measurements of FISH signals. Fluorescence signal intensity per individual nucleus or FISH signals is measured per high power field (×400)and ranked according to increasing fluorescence signal intensity. For measurements of fluorescence intensity see Material and methods. (*a*) Histograms illustrating HPV integrated fluorescence (IF, arbitrary units) in selected nuclei present in basal/parabasal and superficial cell layers processed following either the mild or the harsh protocol (case 2). For representative high power fields, in which the IF was measured, see Figure 1*b* (capture time 0.2 sec) and 1*c* (capture time 3 sec) for the mild and harsh pretreatment methods, respectively. (*b*) Plot for HPV hybridization signals using the mild and harsh protocols in 2 corresponding areas of serial tissue sections (case 19). For representative high power fields, in which the fluorescence signal intensity was measured, see Figure 1*j* and *k* for the mild and harsh pretreatment methods, respectively. (*c*) Plot for HPV hybridization signals in 2 corresponding areas in serial tissue sections pretreated with the mild and harsh protocol exhibiting a typical punctate pattern (case 28). Many nuclei exhibited 2 discrete punctate signals, 1 large and 1 small fluorescent signal. For representative high power field, in which the signals were measured, see figures 1*p* and *q* for the mild and harsh pretreatment methods, respectively. (*d*) Plot for centromere repeat sequence (1q12) hybridization spots in 2 lesions, within 2 different high power fields (case 2: area 1 and 2, case 28: area 3 and 4). For a representative high power field, in which the signals were measured, see Figure 1*d*.

cial layers of the epithelium and so does the fluorescence intensity per individual nucleus (Fig. 1*h*). The majority of the other lesions did not show the clear-cut diffuse pattern in the superficial layer. Utilizing the mild protocol, a granular pattern was often seen in these cases, signals being frequently heterogeneous in size and intensity (Fig, 1*j*). Sometimes these granular patterns were localized to the lower compartment of the epithelium, but in other cases they were scattered throughout the whole of the epithelium. This granular pattern correlated with RNA synthesis as shown by omission of DNA denaturation or by including the RNAse digestion step. Further analysis demonstrated that these RNA signals were superimposed onto multiple spots of HPV DNA. These findings indicate that, in these cases, the contribution of HPV RNA to signal intensity is considerable with the mild protocol. The same holds true for the retention of episomal copies of HPV in the mild protocol.

Cases 15–21 (group B). In this group, we recognized with the harsh protocol a punctate pattern that extended from basal to superficial layers. Figure 1*k* shows an example of the results with the harsh protocol, with the number of signals per nucleus varying within a small range (mean 1.3) and with a single discrete signal throughout the entire thickness of the epithelium in 80% of the nuclei. The mild protocol resulted in a more granular/diffuse pattern with very heterogeneous staining throughout the epithelium (see Fig. 1*j*). In these nuclei, the number of signals varied over a wide range (1 to >10, mean 4). Quantification of the fluorescence intensity showed that the intensity of the individual spots in both methods was of comparable intensity and showed no significant difference in average intensity (Fig. 2*b*). The distribution of the intensities of fluorescent HPV signals measured in a high power field is plotted, with the signals being ranked according to increasing fluorescence intensity. More signals can be identified using the mild protocol, but the average intensity per signal differed only slightly when comparing the mild with the harsh protocol, *i.e.*, 5,000 *vs.* 4,500 a.u., respectively.

The contribution of HPV RNA hybridization to the signal was considerable in this group. This resulted in a granular pattern that was seen throughout the epithelial lesion but in none of these cases did positive cells extend from basal to superficial layer. Sometimes several layers within the epithelium showed strong nuclear RNA signals, while in others the distribution was more random.

Cases 22–35 (group C). Typical examples of cases with punctate HPV FISH patterns are shown in Figure 1*m,n*. These images are illustrative for the majority of lesions in which both the mild and the harsh protocol resulted in a punctate pattern. In all these lesions, the positive cells were found throughout the entire thickness of the epithelium (basal to superficial) or occasionally as small homogeneous foci. In 11 of 14 lesions that exhibited a punctate pattern, only 1 HPV signal was seen in each nucleus. In case 28 the nuclei contained additional small FISH signals (1 or 2) next to 1 strong signal in all nuclei throughout the full epithelial layer (see inserts Figure 1*p,q*).

The contribution of RNA to the HPV signal is more easily assessed in this group than in the lesions in groups A and B because these lesions exhibited a discrete single FISH signal. Case 26 exhibited 1 strong FISH signal per nucleus with the mild protocol (not shown). Omitting target denaturation resulted in intense staining as depicted in Figure 1*m*. After RNase treatment and simultaneous denaturation, 1 signal per nucleus was left (Fig. 1*n*) but with a significantly lower intensity than without RNase treatment. In this case, approximately 80% of the signal intensity stems from hybridization to RNA. In 3 squamous lesions (cases 25, 26 and 32) and 1 adenocarcinoma (case 35), RNA contributed significantly to the final signal using the mild procedure, again up to 80%. In these cases the mild protocol produced higher signal intensity than the harsh protocol. It is noteworthy that 3 of these 4 lesions were HPV 18 positive. In the other cases, the difference was not so evident.

In Figure 2*c* (case 28), quantification of the fluorescence intensity showed that the intensities in both methods are comparable, about 280 and 390, respectively. It is difficult to conclude that the somewhat higher intensity using the mild protocol is the direct effect of hybridization to RNA since hybridization to integrated HPV DNA will contribute to the hybridization signal.

Overal we found that RNA contributes significantly to the hybridization signal obtained with the mild protocol and that the harsh protocol removes RNA as a result of the aggressive extraction of nuclear constituents.

Efficiency of chromosomal (DNA) target detection

To show that the harsh protocol does not influence the efficiency of chromosomal target detection, we applied both the mild and the harsh protocol for the detection of chromosome centromeric DNA targets. For this we hybridized DNA centromeric probes to all of the lesions (for example, see Fig. 1*d*) and used the variation in signal intensity between the different lesions as an indicator of the efficacy of both protocols. Comparable reactivity was seen in all lesions with the harsh protocol, with nearly all nuclei reactive and showing strong FISH signals. The autofluorescent background was low, which is an indicator of the efficient removal of proteins from the cytoplasm and nucleus. These experiments confirmed that the harsh protocol in principle is an efficient method to open chromososomal sites. The mild protocol on the other hand was suboptimal for hybridization to chromosomal targets since a comparable intensity to that obtained with the harsh protocol was identified in only about 25% of cases. In the other lesions, the reactivity was strongly variable throughout the lesion and many lesions showed a high level of autofluorescence.

Two lesions were analyzed in detail by measuring the intensity of individual signals. One case was known to show a typical diffuse HPV pattern while the other showed a punctate HPV pattern. About 700 chromosomal centromere FISH signal intensities were measured and the average intensity was not significantly different in these 2 lesions (see Fig. 2*d*).

Frequency of punctate signal pattern in CIN II/III with and without an adjacent microinvasive carcinoma

Although the study was not intended to determine the frequency of a punctate signal pattern in CIN II/III and CIN II/III adjacent to a microinvasive carcinoma, we describe these results here because they add value to our earlier report.[17] In the previous study, 45 other cases were studied using only the harsh protocol. In the present study a punctate pattern was found in 5 of 17 (29%) solitary CIN II/III lesions and in 9 of 11 (82%) lesions with an adjacent microinvasive carcinoma. This shows that the punctate pattern, which is assumed to be an indication of integration of the virus into the genome, correlates strongly with the transition of a premalignant lesion to microinvasive carcinoma ($p < 0.01$). The mild protocol did not discriminate since a punctate pattern was found in 3 of 17 (17%) CIN II/III lesions and 4 of 11 (36%) CIN&mCA.

When the data from our previous study are included, a punctate pattern was seen in 7 of 40 (18%) CIN II/III lesions and in 19 of 21 (90%) CIN&mCA lesions ($p < 0.001$).

Discussion

In our study, we determined the impact of 2 protocols on the recognition of punctate signal pattern by FISH. It is generally accepted that diffuse signals that represent (replicating) episomal HPV can be distinguished from (strong) punctate signals that indicate integrated HPV. The diffuse pattern is found commonly in low grade intraepithelial lesions and the punctate pattern is characteristically present in invasive carcinomas. However, more complex patterns are found in lesions of intermediate grade (CIN II/III) since the associated HPV infections are generally abortive and the full life cycle of the virus is not supported.[2,9] Furthermore the sensitive tyramide amplification methods that allow the detection of single copy HPV particles complicate these patterns. In addition to describing the morphological patterns of HPV FISH signal obtained with tyramide signal amplification systems, our study quantified HPV signals for the first time in different types of high grade CIN lesions and in invasive carcinomas and determined the contribution of HPV RNA hybridization to signal intensity, as well as intensity variations within single nuclei/cells throughout the epithelium. Two different protocols for HPV detection were used: a mild protocol that retained episomal viral copies and RNA more efficiently, and a harsh protocol that was hypothesized to remove protein and RNA extensively and to partly extract episomal HPV copies.

This comparison allowed us 1) to assess the contribution of RNA hybridization to FISH signal intensity and 2) to identify clonally expanded cells harboring a punctate signal (indicative of HPV integration) present throughout the thickness of the epithelium.

Impact of RNA hybridization on HPV signal

The contribution of RNA hybridisation to HPV signal was best illustrated in the cases that exhibited a punctate pattern. In particular, in those lesions where HPV is known to be integrated, as is the case in ACIS and adenocarcinomas, it was noticed that, using the mild protocol, hybridization to HPV RNA was the major contributor to the HPV signal. That this RNA was extracted by the harsh protocol was deduced from experiments on these lesions because the signal intensity for the harsh protocol was comparable with the mild protocol in which RNase treatment had been performed prior to denaturation. In these cases, it cannot be excluded that the harsh protocol detects only integrated HPV DNA, while, in the mild protocol, residual RNA is the major target for hybridization. This is because many reports have shown that additional steps are needed in combination with the mild protocol to open chromosomal sites for efficient hybridization and immunocytochemical detection.[37] So, loss of hybridization efficiency on DNA could be compensated for by hybridization to RNA when the mild protocol is used. The strong RNA signal is consistent with apparent disruption of the *E2* gene, resulting in unregulated overexpression of viral *E6* and *E7* gene products, although this cannot be determined with certainty as we used a total HPV DNA probe.[9]

When analyzed using the mild procedure, the majority of CIN II/III lesions exhibited a mixed diffuse/granular pattern and RNA also contributed significantly to the signal intensity. This resulted in patterns that were best described as granular. The RNA signals were superimposed on multiple small HPV DNA signals: these RNA patterns were inhomogeneous throughout the lesion and were predominantly seen as punctate signals in the lower compartment of the epithelium. This is consistent with the synthesis of E6 and E7 in this part of the epithelium.[9] Whether or not these patterns represent cells in which the virus is integrated can not be determined by FISH12. We can argue either that this indicates integration, although the scattered distribution pattern of these cells is not indicative of clonal outgrowth, or that, in these cells, there is temporary upregulation of RNA synthesis.

Impact of episomal HPV on the recognition of integrated HPV

With respect to the signal patterns, our study, when applying the mild protocol, confirms the findings of Evans *et al*.[13] who applied the mild protocol in combination with a sensitive bright field TSA ISH method. They observed small punctate signals throughout all epithelial layers in nearly all CIN III lesions. In most cases this was combined with a diffuse pattern.

Quantification of the FISH signals in our study showed that, although the patterns were the same in both protocols, the signal intensity in the mild protocol was frequently higher compared to the signal intensities obtained with the harsh protocol. In the lesions with a punctate pattern (group C), this could be attributed to the contribution of RNA (see above). In the other groups of lesions (group A and B), this difference can be ascribed to both extraction of RNA and partial loss of episomal copies in the harsh protocol. It could be argued that this difference can be entirely attributed to RNA hybridisation. However, the observations that 1) after denaturation of a RNase-treated lesion, analyzed using the mild protocol, the intensity was still higher compared to the harsh protocol and 2) chromosomal targets are more efficiently hybridized in the harsh protocol than in the mild protocol, indicating that integrated HPV is unlikely to have been lost in the harsh protocol, argue in our opinion for loss of episomal copies in the harsh protocol. This partial loss of episomal copies is however very difficult to measure because we do not know how many copies per cell are present within the lesion and we have no denominator for the effectiveness of removal of episomal copies. Furthermore, the presence of concatamers of HPV (with a high molecular weight) in these cells, which are likely to be more strongly anchored in the nucleus, complicates this estimation. Evans *et al*.[12] interpreted the punctate signals as integration in all CIN 11/III lesions. Although they emphasize that not all signals represent integrated HPV, all the lesions were classified as HPV integrated lesions. This implies that, in nearly all CIN III lesions, the integrated HPV is hidden in a background of episomal copies.

Our data suggest that this shielding of integrated HPV does occur. However, this was only seen in 7 of 21 CIN II/III lesions and was identified when the lesions were processed following the harsh protocol: the mild protocol was inconclusive in these cases. Furthermore the fact that the punctate pattern was seen throughout the full thickness of the epithelium in these lesions strengthens the assumption that these cells have undergone clonal expansion. It was surprising to see that 5 of these lesions were associated with a microinvasive carcinoma.

One could argue that it is unlikely that these signals represent integrated HPV because more prominent expression of RNA should have been identified in these cases and that this should have resulted, in particular using the mild protocol, in strong punctate signals (as discussed above). A possible explanation for the reduced expression could be that RNA expression is variable or that detection is affected by methodological issues such as, *e.g*., tissue fixation and reproducibility of the pretreatment. An alternative explanation is that the *E2* gene is still intact, suppressing E6/E7 transcription, or that E2 synthesized from episomal copies suppresses the E6/E7 from integrated virus.[38] The latter has been demonstrated by transfection of *E2* into cell lines containing integrated HPV.

Frequency of integration in CIN II/III

In a previous study, we found that the punctate signal pattern, and by implication integration of HPV, in CIN II/III lesions, as assessed by FISH, correlated with the presence of a microinvasive carcinoma ($p < 0.001$)[17]. Although the present study was not designed to validate this observation further, the same significant correlation was found ($p < 0.01$) when utilizing the harsh protocol in the newly selected cases. Combining the data from both studies, 7 of 40 (18%) solitary CIN II/III lesions showed a clonally expanded population of cells containing integrated HPV. In the series of CIN III lesions adjacent to a microinvasive carcinoma, integration dominated and was shown in 9 of 11 cases. Consistent with these findings, several earlier studies state that integration of HPV, detected by PCR or FISH, occurs preferentially in association with invasion and is relatively uncommon in noninvasive intraepithelial neoplasms.[19,39,40]

Recently Wentzensen *et al*.[39–43] reviewed the genomic integration sites of HPV in epithelial dysplasia and invasive cancer as determined by means of direct HPV DNA integration methods as well as the amplification of papillomavirus oncogene transcripts (APOT) assay. By means of these assays, a total of 192 individual HPV integration sites have been reported; approximately 180 of these sites were determined in invasive carcinomas, while the site of HPV integration was determine in only 10 CIN III lesions. In these CIN III lesions, the APOT assay was used in combination with an extensive comparative database search to identify the genomic location. In these cases, there is direct (biochemical) proof of integration into the genome determined by the presence of a RNA fusion product. Our observation that the cells with a punctate pattern (after application of the harsh protocol) are present throughout the whole epithelial layer supports the view that cervical epithelia expressing chromosomally integrated HPV oncogenes have a strong selective growth advantage.[41,44]

The frequency at which these punctate staining patterns are detected in our study in solitary CIN II/III is in line with the data (frequencies) obtained by the group of von Knebel Doeberitz,[40,45] who detected integration of HPV by means of PCR amplification of viral transcripts (APOT assay: 4.5–5% CIN II; 14–15.6% CIN III) and Kalantari *et al*.[39] who applied an inverse polymerase chain reaction (5% CIN III, rliPCR) assay. These studies point to the marked difference between the prevalence of integration in CIN II/III lesions and invasive carcinomas, and confirm the data obtained using Southern blot analysis.[46].

In contrast, several other studies report that viral integration is common in CIN II/III. By use of a PCR protocol, measuring E2/E6 DNA ratio, Peitsaro *et al*.[47] measured ratios between episomal/integrated HPV copies of about 1.0 (or lower) in nearly all CIN II/III lesions. There is no obvious methodological reason for the discrepancy between these data and those obtained using APOT and rliPCR, although, *e.g*., choice of primer, length of amplicon and quality of material (frozen *vs*. paraffin embedded material) will influence the efficiency of the assay. The duration of the disease, and hence the frequency of integration, may also be different in various studies. Furthermore, in HPV DNA concatamers, E2 DNA sequences could be lost, while no RNA is synthesized. The latter would result in an apparent discrepancy because loss of E2 would lead to classification as ''integrated'' HPV using the E2/E6 assay, while the absence of RNA (fusion product) would lead to classification as ''nonintegrated'' using the APOT assay.

Taken together, the exact frequency of viral integration in CIN II/III on the basis of PCR and (F)ISH data is open to question. Comparison of data obtained using several of the DNA integration methods described above, targeting HPV DNA and RNA in the same tissue material, is required to answer this ''frequency'' question in CIN II/III. We believe, however, that integrated HPV can

be detected efficiently using the harsh protocol and scoring of punctate signals. For the identification of HPV, and HPV typing, the mild protocol is beneficial since this protocol detects HPV RNA and most probably most of the episomal HPV copies.

We conclude that scoring of punctate HPV FISH signals is a suitable molecular marker for detection of CIN II/III at risk for progression to invasive carcinoma. Since punctate signal, and by implication viral integration, correlates strongly with the presence of invasive carcinoma, the screening of cytological specimens from high-grade lesions by HPV FISH with determination of the signal pattern could represent an auxiliary strategy to standard screening methods. However, the pretreatment procedure used for ISH is extremely important because episomal copies, as well as RNA, will produce morphologically localized signals that can be misinterpreted as integrated virus. The concepts presented in our study could help to design an optimal procedure and help classification of HPV patterns.

Acknowledgements

The authors thank F. Kwaspen for providing the HPV probes.

References

1. Crum CP. Contemporary theories of cervical carcinogenesis: the virus, the host, and the stem cell. Mod Pathol 2000;13:243–51.
2. zur Hausen H. Papillomaviruses and cancer: from basic studies to clinical application. Nat Rev Cancer 2002;2:342–50.
3. Ferenczy A, Franco E. Persistent human papillomavirus infection and cervical neoplasia. Lancet Oncol 2002;3:11–6.
4. von Knebel Doeberitz M. New markers for cervical dysplasia to visualise the genomic chaos created by aberrant oncogenic papillomavirus infections. Eur J Cancer 2002;38:2229–42.
5. Ostor AG, Mulvany N. The pathology of cervical neoplasia. Curr Opin Obstet Gynecol 1996;8:69–73.
6. Nobbenhuis MA, Walboomers JM, Helmerhorst TJ, Rozendaal L, Remmink AJ, Risse EK, van der Linden HC, Voorhorst FJ, Kenemans P, Meijer CJ. Relation of human papillomavirus status to cervical lesions and consequences for cervical-cancer screening: a prospective study. Lancet 1999;354:20–5.
7. Ziegert C, Wentzensen N, Vinokurova S, Kisseljov F, Einenkel J, Hoeckel M, von Knebel Doeberitz M. A comprehensive analysis of HPV integration loci in anogenital lesions combining transcript and genome-based amplification techniques. Oncogene 2003;22:3977–84.
8. Wentzensen N, Ridder R, Klaes R, Vinokurova S, Schaefer U, Doeberitz MK. Characterization of viral-cellular fusion transcripts in a large series of HPV16 and 18 positive anogenital lesions. Oncogene 2002;21:419–26.
9. Middleton K, Peh W, Southern S, Griffin H, Sotlar K, Nakahara T, El-Sherif A, Morris L, Seth R, Hibma M, Jenkins D, Lambert P, et al. Organization of human papillomavirus productive cycle during neoplastic progression provides a basis for selection of diagnostic markers. J Virol 2003;77:10186–201.
10. Riley RR, Duensing S, Brake T, Munger K, Lambert PF, Arbeit JM. Dissection of human papillomavirus E6 and E7 function in transgenic mouse models of cervical carcinogenesis. Cancer Res 2003;63:4862–71.
11. Schaeffer AJ, Nguyen M, Liem A, Lee D, Montagna C, Lambert PF, Ried T, Difilippantonio MJ. E6 and E7 oncoproteins induce distinct patterns of chromosomal aneuploidy in skin tumors from transgenic mice. Cancer Res 2004;64:538–46.
12. Evans MF, Cooper K. Human papillomavirus integration: detection by in situ hybridization and potential clinical application. J Pathol 2004;202:1–4.
13. Evans MF, Mount SL, Beatty BG, Cooper K. Biotinyl-tyramide-based in situ hybridization signal patterns distinguish human papillomavirus type and grade of cervical intraepithelial neoplasia. Mod Pathol 2002; 15:1339–47.
14. Rihet S, Lorenzato M, Clavel C. Oncogenic human papillomaviruses and ploidy in cervical lesions. J Clin Pathol 1996;49:892–6.
15. Lizard G, Chignol MC, Souchier C, Schmitt D, Chardonnet Y. Laser scanning confocal microscopy and quantitative microscopy with a charge coupled device camera improve detection of human papillomavirus DNA revealed by fluorescence in situ hybridization. Histochemistry 1994;101:303–10.
16. Ziol M, Di Tomaso C, Biaggi A, Tepper M, Piquet P, Carbillon L, Uzan M, Guettier C. Virological and biological characteristics of cervical intraepithelial neoplasia grade I with marked koilocytotic atypia. Hum Pathol 1998;29:1068–73.
17. Hopman AH, Smedts F, Dignef W, Ummelen M, Sonke G, Mravunac M, Vooijs GP, Speel EJ, Ramaekers FC. Transition of high-grade cervical intraepithelial neoplasia to micro-invasive carcinoma is characterized by integration of HPV 16/18 and numerical chromosome abnormalities. J Pathol 2004;202:23–33.
18. Sano T, Hikino T, Niwa Y, Kashiwabara K, Oyama T, Fukuda T, Nakajima T. In situ hybridization with biotinylated tyramide amplification: detection of human papillomavirus DNA in cervical neoplastic lesions. Mod Pathol 1998;11:19–23.
19. Cooper K, Herrington CS, Stickland JE, Evans MF, McGee JO. Episomal and integrated human papillomavirus in cervical neoplasia shown by non-isotopic in situ hybridisation. J Clin Pathol 1991; 44:990–6.
20. Adler K, Erickson T, Bobrow M. High sensitivity detection of HPV-16 in SiHa and CaSki cells utilizing FISH enhanced by TSA. Histochem Cell Biol 1997;108:321–4.
21. Hafkamp HC, Speel EJ, Haesevoets A, Bot FJ, Dinjens WN, Ramaekers FC, Hopman AH, Manni JJ. A subset of head and neck squamous cell carcinomas exhibits integration of HPV 16/18 DNA and overexpression of p16INK4A and p53 in the absence of mutations in p53 exons 5–8. Int J Cancer 2003;107:394–400.
22. Kerstens H, Poddighe P, Hanselaar A. A novel in situ hybridization signal amplification method based on the deposition of biotinylated tyramine. J Histochem Cytochem 1995;43:347–52.
23. Player AN, Shen LP, Kenny D, Antao VP, Kolberg JA. Single-copy gene detection using branched DNA (bDNA) in situ hybridization. J Histochem Cytochem 2001;49:603–12.
24. Plummer TB, Sperry AC, Xu HS, Lloyd RV. In situ hybridization detection of low copy nucleic acid sequences using catalyzed reporter deposition and its usefulness in clinical human papillomavirus typing. Diagn Mol Pathol 1998;7:76–84.
25. Kenny D, Shen LP, Kolberg JA. Detection of viral infection and gene expression in clinical tissue specimens using branched DNA (bDNA) in situ hybridization. J Histochem Cytochem 2002;50:1219–27.
26. Stoler MH, Broker TR. In situ hybridization detection of human papillomavirus DNAs and messenger RNAs in genital condylomas and a cervical carcinoma. Hum Pathol 1986;17:1250–8.
27. Hopman AH, Kamps MA, Speel EJ, Schapers RF, Sauter G, Ramaekers FC. Identification of chromosome 9 alterations and p53 accumulation in isolated carcinoma in situ of the urinary bladder versus carcinoma in situ associated with carcinoma. Am J Pathol 2002;161:1119–25.
28. Veltman JA, Bot FJ, Huynen FC, Ramaekers FC, Manni JJ, Hopman AH. Chromosome instability as an indicator of malignant progression in laryngeal mucosa. J Clin Oncol 2000;18:1644–51.
29. Park JS, Hwang ES, Park SN, Ahn HK, Um SJ, Kim CJ, Kim SJ, Namkoong SE. Physical status and expression of HPV genes in cervical cancers. Gynecol Oncol 1997;65:121–9.
30. Cooke HJ, Hindley J. Cloning of human satellite III DNA: different components are on different chromosomes. Nucleic Acids Res 1979;6:3177–97.
31. Waye JS, Willard HF. Molecular analysis of a deletion polymorphism in alpha satellite of human chromosome 17: evidence for homologous unequal crossing-over and subsequent fixation. Nucleic Acids Res 1986;14:6915–27.
32. Hopman AHN, FCS R. Processing and staining of cell and tissue material for interphase cytogenetics. New York: John Wiley & Sons, Inc., 1998.
33. Speel EJ, Ramaekers FC, Hopman AH. Sensitive multicolor fluorescence in situ hybridization using catalyzed reporter deposition (CARD) amplification. J Histochem Cytochem 1997;45:1439–46.
34. Speel EJ, Hopman AH, Komminoth P. Amplification methods to increase the sensitivity of in situ hybridization: play card(s). J Histochem Cytochem 1999;47:281–8.
35. Nederlof PM, van der Flier S, Raap AK, Tanke HJ. Quantification of inter- and intra-nuclear variation of fluorescence in situ hybridization signals. Cytometry 1992;13:831–8.
36. Hopman AH, Ramaekers FC, Speel EJ. Rapid synthesis of biotin-, digoxigenin-, trinitrophenyl-, and fluorochrome-labeled tyramides and their application for in situ hybridization using CARD amplification. J Histochem Cytochem 1998;46:771–7.
37. Evans MF, Aliesky HA, Cooper K. Optimization of biotinyl-tyramide-based in situ hybridization for sensitive background-free applications on formalin-fixed, paraffin-embedded tissue specimens. BMC Clin Pathol 2003;3:2.
38. Bechtold V, Beard P, Raj K. Human papillomavirus type 16 E2 protein has no effect on transcription from episomal viral DNA. J Virol 2003;77:2021–8.
39. Kalantari M, Blennow E, Hagmar B, Johansson B. Physical state of HPV16 and chromosomal mapping of the integrated form in cervical carcinomas. Diagn Mol Pathol 2001;10:46–54.

40. Klaes R, Woerner SM, Ridder R, Wentzensen N, Duerst M, Schneider A, Lotz B, Melsheimer P, von Knebel Doeberitz M. Detection of high-risk cervical intraepithelial neoplasia and cervical cancer by amplification of transcripts derived from integrated papillomavirus oncogenes. Cancer Res 1999;59:6132–6.
41. Wentzensen N, Vinokurova S, von Knebel Doeberitz M. Systematic review of genomic integration sites of human papillomavirus genomes in epithelial dysplasia and invasive cancer of the female lower genital tract. Cancer Res 2004;64:3878–84.
42. Thorland EC, Myers SL, Persing DH, Sarkar G, McGovern RM, Gostout BS, Smith DI. Human papillomavirus type 16 integrations in cervical tumors frequently occur in common fragile sites. Cancer Res 2000;60:5916–21.
43. Luft F, Klaes R, Nees M, Durst M, Heilmann V, Melsheimer P, von Knebel Doeberitz M. Detection of integrated papillomavirus sequences by ligation-mediated PCR (DIPS-PCR) and molecular characterization in cervical cancer cells. Int J Cancer 2001;92:9–17.
44. Jeon S, Allen-Hoffmann BL, Lambert PF. Integration of human papillomavirus type 16 into the human genome correlates with a selective growth advantage of cells. J Virol 1995;69:2989–97.
45. Melsheimer P, Vinokurova S, Wentzensen N, Bastert G, von Knebel Doeberitz M. DNA aneuploidy and integration of human papillomavirus type 16 e6/e7 oncogenes in intraepithelial neoplasia and invasive squamous cell carcinoma of the cervix uteri. Clin Cancer Res 2004; 10:3059–63.
46. Cullen AP, Reid R, Campion M, Lorincz AT. Analysis of the physical state of different human papillomavirus DNAs in intraepithelial and invasive cervical neoplasm. J Virol 1991;65:606–12.
47. Peitsaro P, Johansson B, Syrjanen S. Integrated human papillomavirus type 16 is frequently found in cervical cancer precursors as demonstrated by a novel quantitative real-time PCR technique. J Clin Microbiol 2002;40:886–91.